

## Kirkendall effect induced hollow structured materials for energy storage application

LING Dandan<sup>1</sup>, WANG Qi<sup>1</sup>, ZHANG Daohong<sup>1,2</sup>, WANG Qiufan<sup>1,2\*</sup>

(1 South-Central Minzu University, a. Key Laboratory of Catalysis and Energy Materials Chemistry of Ministry of Education & Hubei Key Laboratory of Catalysis and Materials Science; b. Hubei R&D Center of Hyperbranched Polymers Synthesis and Applications, Wuhan 430074, China; 2 Guangdong Provincial Laboratory of Chemistry and Fine Chemical Engineering Jieyang Center (Rongjiang Laboratory of Guangdong Province), Jieyang 515200, Guangdong China)

**Abstract** Materials engineering plays a key role in the field of electrochemical energy storage, and considerable efforts have been made in recent years to fulfill the future requirements of electrochemical energy storage using novel functional electrode materials. Materials with hollow structures are of particular interests due to their low density, large specific surface area and high porosity, making them promising candidates for energy conversion and storage. The Kirkendall effect has been widely applied for the synthesis of nanoscale hollow structures, which involves an unbalanced counter diffusion through a reaction interface. Herein, the recent progress on the use of the nanoscale Kirkendall effect to synthesize hollow nanostructures, including nanoparticles, one-dimensional (1-D), two-dimensional (2-D), and three-dimensional (3-D) nanostructures, and their potential applications in energy storage devices are summarized and discussed. And prospects is made for the future development of this research field.

**Keywords** Kirkendall effect; hollow structure; energy storage devices

中图分类号 O6-1 文献标志码 A 文章编号 1672-4321(2025)06-0721-17

doi:10.20056/j.cnki.ZNMDZK.20250601

## Kirkendall效应诱导空心结构材料在储能领域的应用

凌丹丹<sup>1</sup>, 王琪<sup>1</sup>, 张道洪<sup>1,2</sup>, 王秋凡<sup>1,2\*</sup>

(1 中南民族大学 a. 催化转化与能源材料化学教育部重点实验室暨催化材料科学湖北省重点实验室; b. 超支化聚合物合成与应用技术湖北省工程研究中心, 武汉 430074; 2 化学与精细化工广东省实验室揭阳分中心 (广东省榕江实验室), 广东 揭阳 515200)

**摘要** 材料工程在电化学储能领域发挥着关键作用, 近年来已经使用相当多的努力构建新型功能电极材料以满足电化学储能的未来要求. 中空结构材料因其低密度、大比表面积和高孔隙率等而引起特别关注, 使其成为能量转换和存储的潜在候选材料. Kirkendall效应已广泛应用于纳米空心结构的合成, 该效应涉及通过反应界面的不平衡反向扩散. 总结和讨论了利用纳米基尔肯达尔效应合成空心纳米结构的最新进展, 包括一维(1-D)、二维(2-D)和三维(3-D)纳米颗粒及其在储能器件中的潜在应用, 并对该研究领域的未来发展进行了展望.

**关键词** Kirkendall效应; 中空结构; 储能器件

The global energy crisis and environmental pollution are considered as the two biggest challenges in the 21st century, so there is an urgent need for clean, renewable and sustainable energy sources. With the ever-increasing demands to support newly emerging electronics, scientists pay great efforts to

develop next-generation electrochemical energy storage (EESs) with large capacity, high safety, high stability and rate capability. The performance of the EES system largely depends on the properties of the electrode materials. Hollow and porous structures have been attracting extensive research interest on account

收稿日期 2024-01-25

\* 通信作者 王秋凡(1988-), 女, 副教授, 博士, 研究方向: 新能源材料与器件, Email: ygdf@mail.scuec.edu.cn

基金项目 国家自然科学基金资助项目(51702369, U23A20691); 武汉知识创新项目-曙光计划资助项目(2023010201020467)

of their advantages including low density, large specific surface area and high porosity<sup>[1]</sup>. Hollow micro/nanostructures have a larger ion-accessible surface area than solid ones, and thus can improve the utilization of the active materials, and are favorable for electrochemical energy storage applications. A number of synthetic routes to porous, hollow nanomaterials have been reported, they can be divided into template method and non-template method<sup>[1-3]</sup>.

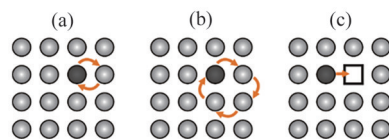
For template method, many approaches for hollow structures is to fabricate the core/shell intermediate using a hard template and then removing the hard solid template, or to use a solid reactant itself as a sacrificial template<sup>[4-5]</sup>. Furthermore, hollow structures can be obtained at the interface between discontinuous emulsion droplets/supramolecular micelles and continuous fluid phase using liquid droplets/micelles as a soft template<sup>[6-7]</sup>. Hollow nanostructures are obtained *via* nano-templates methods usually using Ostwald ripening and Kirkendall effect. For Ostwald ripening process, during the recrystallization of crystallites, mass transfer from smaller crystallites in the core region to larger crystallites in the shell region of the crystallite aggregate intermediate led to a hollow structure without relying on the external template<sup>[8-11]</sup>. The hollow nanocrystal can be synthesized using a solid reactant as a sacrificial template through the Kirkendall effect, wherein, the hollow cavity forms near the interface between two reactants, due to different interdiffusion rates of the two reactants<sup>[12]</sup>. Ji *et al.*<sup>[13]</sup> prepared hollow  $\text{Co}_3\text{O}_4$  nanoparticles with rich oxygen vacancies which was formed and controlled through the regulation of Kirkendall effect. To further study the nanoscale Kirkendall effect, NILSSON *et al.*<sup>[14]</sup> developed a combined experimental and theoretical platform for the investigation of single Cu nanoparticles oxidation and Kirkendall void formation.

However, there is still no specific summary focusing on the nanoscale Kirkendall effect to hollow nanocrystal. This review summarized and analysed the recent progress in the synthesis of hollow structures and the use of them in energy storage application as electrode materials. The review begins with a brief introduction of the nanoscale Kirkendall effect, and

then discusses the recent research of hollow materials based on nanoscale Kirkendall effect in energy storage, lastly concludes with a summary and the personal perspectives on the directions in which future work on this field might be focused.

## 1 Kirkendall effect

The Kirkendall effect is a classical phenomenon in metallurgy, which refers to a nonequilibrium mutual diffusion process through an interface of two metals so that vacancy diffusion occurs to compensate for the unequal material flow. Prior to 1940s, it was believed that atomic diffusion in metals and alloys took place *via* a direct exchange or ring mechanism (Fig.1 (a), (b)). However, 1942, Kirkendall explained the interdiffusion between copper and zinc in a copper/brass system, the experimental data supported the theory that atomic interdiffusion at the interface of two metals occurs through a vacancy exchange mechanism (Fig.1(c))<sup>[15]</sup>.

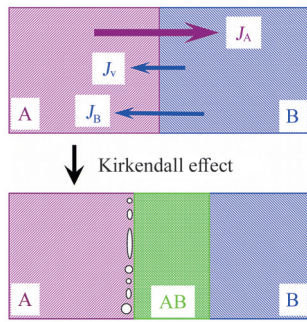


(a) Direct exchange mechanism; (b) Ring mechanism; (c) Vacancy mechanism (Figure adapted with permission from literature [15], copyright 1997 Springer Science and Business Media)

Fig. 1 Schematic diagram of atomic diffusion  
图1 原子扩散示意图

Fig. 2 demonstrates the schematic illustration of the Kirkendall effect in the bulk phase diffusion couple A-B<sup>[12]</sup>. Due to the faster diffusion of A into B than that of B into A, the unequal material flow is accompanied by vacancy diffusion. In this case, the A-B alloy region will be more extended within metal B and vacancies will be injected at the interface region within metal A. The coalescence of excess of vacancies leads to the formation of small voids distributed all along the interface. The process goes on over time, vacancies will be generated leading to the enlargement of the formed voids that will coalesce and form pores within the materials.

The final morphology of the reaction product is dependent on many factors including the crystal structure, crystal defects, grain size, concentration of the reactants, and reaction temperature<sup>[16]</sup>. Hollow



$J_A$ ,  $J_B$  and  $J_V$  are diffuse fluxes of metal A, B, and void, respectively. (Figure adapted with permission from literature [12], copyright 2012 American Chemical Society)

Fig. 2 Schematic illustration of a nonequilibrium lattice diffusion at the interface in bulk phase by Kirkendall effect

图2 Kirkendall效应导致的体相界面非平衡晶格扩散示意图

structures may be obtained when the diffusion couple is properly chosen and the reaction kinetics is facilitated by lower activation energy such as surface diffusion and interface strain<sup>[17-18]</sup>. Hollow nanostructures can offer more active sites for electrochemical reactions and short ionic transport paths, which provide the enhanced rate capability and cycle performance.

The research on the nanoscale Kirkendall effect is newly developed field and many progressive breakthroughs have been made in this field (Fig. 3). The ion-exchange process is an effective method to obtain hollow nanostructure based on the nanoscale Kirkendall effect<sup>[19-20]</sup>. In addition, Specific metal doping in the crystal will also influence the Kirkendall effect. GURIA *et al.*<sup>[21]</sup> demonstrated that Ag doping in Pd nanocrystals triggered the Kirkendall effect during the subsequent selenization process, which could not occur in the undoped sample. Multi-component hollow nanomaterials with different microscopic morphologies can be obtained by combining the nanoscale Kirkendall effect with metal-organic frameworks (MOFs) strategy, sacrificial template method, self-assembly, etc. WANG *et al.*<sup>[22]</sup> successfully synthesized a hollow porous layered  $\text{CoMn}_2\text{O}_4@\text{NC}$  microbox for lithium ion storage by using kirkendall effect and self-assembly. The  $\text{CoMn}_2\text{O}_4$  micro-box shows a dense skin, porous interior and unique cavity, which is beneficial to adapt to volume change and promote electrolyte penetration.  $\text{CoMn}_2\text{O}_4@\text{NC}$  has a high specific capacity of  $1039 \text{ mAh}\cdot\text{g}^{-1}$  after 150 cycles at  $0.5 \text{ A}\cdot\text{g}^{-1}$ .

## 2 Synthesis of hollow nanostructures

Controlling the morphology and size of hollow structure is vital to their applications. In the review, we will focus on the nanoscale Kirkendall effect to synthesize hollow structure for specific geometric morphologies, including nanoparticles, 1-D, 2-D and 3-D structures and their application of energy storage.

### 2.1 Nanoparticles

In the formation process of nanomaterials, large-volume nanocrystals can be dispersed into extremely small nanoparticles by external application of energy, and ultrasmall nanoparticles can be obtained through the restricted growth of the shell. The size of uniformly dispersed nanoparticles is usually less than 100 nm. Ultrasmall hollow nanostructures can promote much faster charge transport and expose more active sites as well as migrate the volume change stress more efficiently than the solid and large hollow counterparts, thus demonstrating remarkable electrochemical energy storage performance.

Transition-metal oxides (TMOs), with rich redox behavior and low cost, have been widely studied and used in the field of energy storage and conversion<sup>[23]</sup>. JI *et al.*<sup>[13]</sup> reported the tuning of oxygen vacancy in the embedded hollow  $\text{Co}_3\text{O}_4$  nanoparticles on the freestanding hierarchically porous carbon micro-structure through the regulation of nanoscale Kirkendall effect. Fig.4 (a) - (d) demonstrate the embedded Co particles in Co NPs@HPNCS (Co nanoparticle@hierarchically porous N-doped carbon structure) under a solid→yolk→shell→hollow evolution process during the 90 min oxidation treatment, suggesting the proceeding of a slow Kirkendall and diffusion process. The Kirkendall effect on engineering oxygen vacancy is shown in Fig.4 (e). Due to the slow kinetics of oxygen and carbon in metals, the unbalanced diffusion rate leads to the migration of oxygen vacancies, and finally the hollow nanoparticle structure is formed. Therefore, people can customize different structures by using the Kirkendall effect on unique structures and simply controlling the oxidation time. In addition to oxides, transition-metal selenides have attracted much attention as promising anode materials for energy

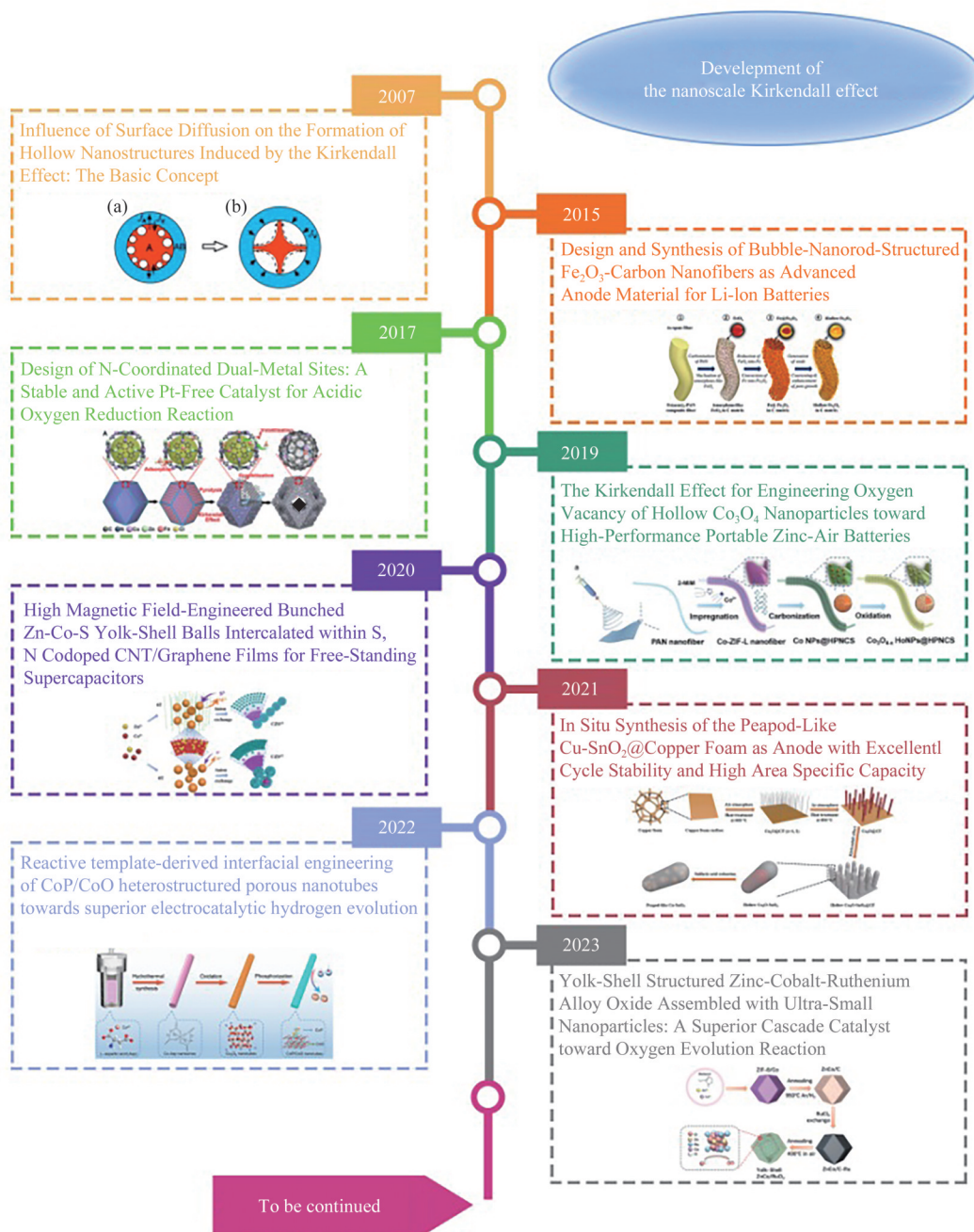


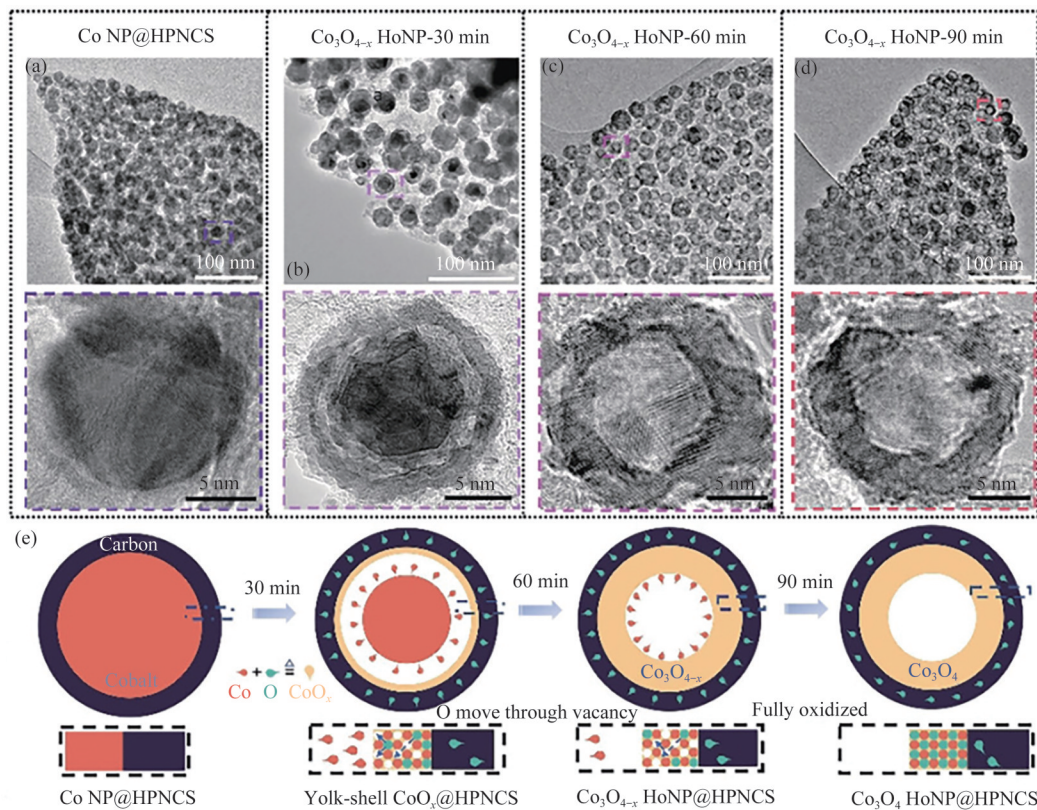
Fig. 3 Timeline of major progresses for the development of nanoscale Kirkendall effect

图3 纳米级 Kirkendall 效应主要的发展时间表

storage by virtue of their high capacity, chemical stability, and low environmental impact. TANG *et al.*<sup>[24]</sup> exhibited a novel strategy to delicately synthesize cellular carbon-wrapped  $\text{FeSe}_2$  nanocavities ( $\text{h-FeSe}_2$ @PC) with sub-5 nm ultrathin walls and multiple rooms for ultrafast sodium storage.  $\text{Fe}_3\text{C}$ @PC was obtained by pyrolyzing the raw material PVP-chelated  $\text{Fe}(\text{NO}_3)_3$ . Then it was selenized at different times (such as 2, 4, and 8 h). With the extension of selenization time to 8 h, the  $\text{FeSe}_2$  in  $\text{h-FeSe}_2$ @PC-8h

eventually develop to give an ultrathin-wall multiroom superstructure.

MOFs are composed of metal nodes and organic bonds through strong coordination bonds. They have rich characteristics such as porous crystal framework, ultra-high porosity and specific surface area, adjustable composition and structural height. It is often used as a precursor to manufacture hollow nanomaterials in the synthesis of electrode materials<sup>[25-26]</sup>. FAN *et al.* reported that ultrafine MOF nanocrystals were



(a)-(d) Time-dependent TEM images; (e) Illustration of the evolution of Co particles into hollow Co<sub>3</sub>O<sub>4</sub> particles with the formation of oxygen vacancies during the oxidation process (Figure adapted with permission from literature [13], copyright 2019 Wiley)

Fig. 4 Kirkendall effect of nanoparticles

图4 纳米颗粒的kirkendall效应

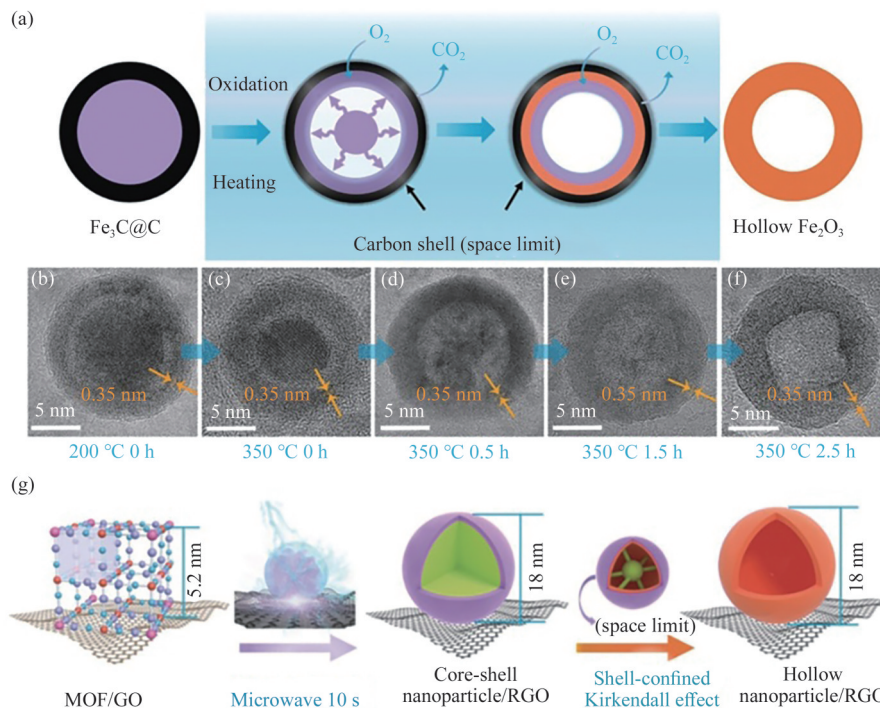
uniformly grown on graphene by microwave-assisted and Kirkendall effect as precursors to prepare ultrafine hollow nanoparticles<sup>[27]</sup>. In this study, the outward diffusion of core materials is accompanied by the inward diffusion of vacancies from carbon shell to core and the inward diffusion of oxygen along carbon shell. Subsequently, Fe<sub>3</sub>C diffuses all the way in the carbon shell, and even passes through the carbon shell to react with oxygen, and the carbon shell is slowly consumed in this process (Fig. 5 (a)). As shown in Fig. 5(b)-(f), although the carbon layer with an interlayer spacing of 0.35 nm is continuously consumed during the oxidation process, the core is always wrapped by the carbon layer until the hollow Fe<sub>2</sub>O<sub>3</sub> nanostructure is completely formed. Therefore, the carbon layer not only acts as a reaction interface between oxygen and iron, but also acts as a template in the oxidation process, which has a space restriction effect in the transformation process to limit the size and excessive growth of hollow nanoparticles. It is worth

noting that H-Fe<sub>2</sub>O<sub>3</sub>/RGO exhibits a reversible capacity of 684 mAh·g<sup>-1</sup> at 5 A·g<sup>-1</sup>, achieving super-high lithium ion storage performance.

## 2.2 1-D hollow nanostructures

The continuous network in 1-D nanostructures including nanowires, nanorods, and nanotubes etc. can act as the “highway” for charge transport along their longitudinal direction and the shortened ion diffusion length in 1-D nanostructures results in the increase of rate performance when applied in electrochemical energy storage devices. Moreover, 1-D nanostructures with relatively large surface areas, can form porous network microstructure that acts as the scaffold/support of metal oxides, which facilitates the mass transport of the solvated ions in the electrolyte to the surface of electrodes<sup>[28]</sup>.

Nanowires are considered as promising materials for energy-related applications, with high surface area ratio and large active interface between electrolyte and electrode, which can be used as electron channels for



(a) Formation mechanism and conversion process of hollow  $\text{Fe}_2\text{O}_3$  nanoparticles derived from core-shell  $\text{Fe}_3\text{C}@\text{C}$  nanoparticles by the shell-confined Kirkendall diffusion effect; (b)-(f) TEM images of the products annealing in the air at different stages of (b)  $200\text{ }^\circ\text{C}$  0 h, (c)  $350\text{ }^\circ\text{C}$  0 h, (d)  $350\text{ }^\circ\text{C}$  0.5 h, (e)  $350\text{ }^\circ\text{C}$  1.5 h, (f)  $350\text{ }^\circ\text{C}$  2.5 h; (g) Illustration of the synthesis process of the hollow nanoparticles/RGO (Figure adapted with permission from literature [27], copyright 2020 Wiley)

Fig. 5 Kirkendall effect of MOF-derived nanoparticles

图5 由MOF衍生的纳米颗粒的Kirkendall效应

efficient charge transfer<sup>[29]</sup>. LI *et al.*<sup>[30]</sup> constructed an ultrafine Ag/MnO<sub>x</sub> nanowire structure for supercapacitors. Hairy nanostructures promote rapid ion diffusion (high specific surface area) at the electrode/electrolyte interface and electron transfer in the channel, which makes them provide theoretically high specific capacitance. BANDYOPADHYAY *et al.*<sup>[31]</sup> studied the preparation method of multilevel Zn-Ni-Co-S nanowire arrays. Firstly, Zn-Ni-Co Hp nanowire arrays were prepared directly on nickel foam by hydrothermal reaction. During the secondary hydrothermal sulfidation, due to the Kirkendall effect, the diffusion rate of metal cations to the surface is relatively higher than that of sulfide ions, which leads to the formation of cavities inside nanowires. The energy density can reach  $88.6\text{ Wh}\cdot\text{kg}^{-1}$  when it is used in solid-state asymmetric supercapacitors.

Nanorods, as 1-D nanomaterials, have been widely concerned by researchers in recent years<sup>[32]</sup>. HUANG *et al.*<sup>[33]</sup> designed a FR-FeOOH nanorod for high-performance sodium storage. The cavity formed by Kirkendall effect provides abundant channels and

enough space for ion transport to alleviate volume expansion, showing excellent  $\text{Na}^+$  storage performance (high capacity of  $210\text{ mAh}\cdot\text{g}^{-1}$  at  $0.8\text{ A}\cdot\text{g}^{-1}$ ). PARK *et al.*<sup>[34]</sup> proposed a new mechanism to transform metal selenides with hierarchical structure into their corresponding metal oxides with unique structures through Kirkendall effect. In order to further understand this phenomenon, the detailed formation mechanism of porous  $\text{Fe}_2\text{O}_3$  nanorods is proposed in Fig. 6. In the oxidation step, the different diffusion rates of iron cations, selenium components and oxygen lead to several types of intermediate products. Starting from  $\text{FeSe}_2$  nanorod clusters, the  $\text{Se}@\text{FeO}_x$  surface layer with core-shell structure is first formed due to the fast diffusion rate of iron ions. Subsequently, the nano-porous Se layer is melted to produce a porous structure permeable to oxygen. Iron cations further diffuse outward to form a  $\text{Fe}_2\text{O}_3$  layer on the external Se layer.  $\text{FeSe}_2$  was completely transformed into  $\text{FeO}_x$ , and porous  $\text{FeO}_x$ -Se nanorods were obtained. Finally, the evaporation of  $\text{SeO}_2$  layer and the oxidation of  $\text{FeO}_x$

at low boiling point produce porous  $\text{Fe}_2\text{O}_3$  nanorods with a large number of interconnected empty nanovoids. The porous structure can permeate the liquid

electrolyte, thus producing a graded  $\text{Fe}_2\text{O}_3$  anode material with long cycle and excellent rate performance.

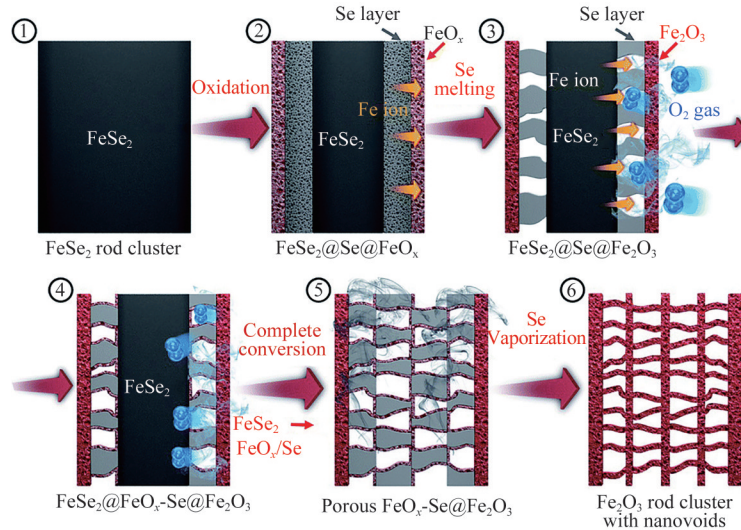


(Figure adapted with permission from literature [34], copyright 2018 The Royal Society of Chemistry)

Fig. 6 Formation mechanism of nanopores in  $\text{Fe}_2\text{O}_3$  nanorod clusters by the Kirkendall effect

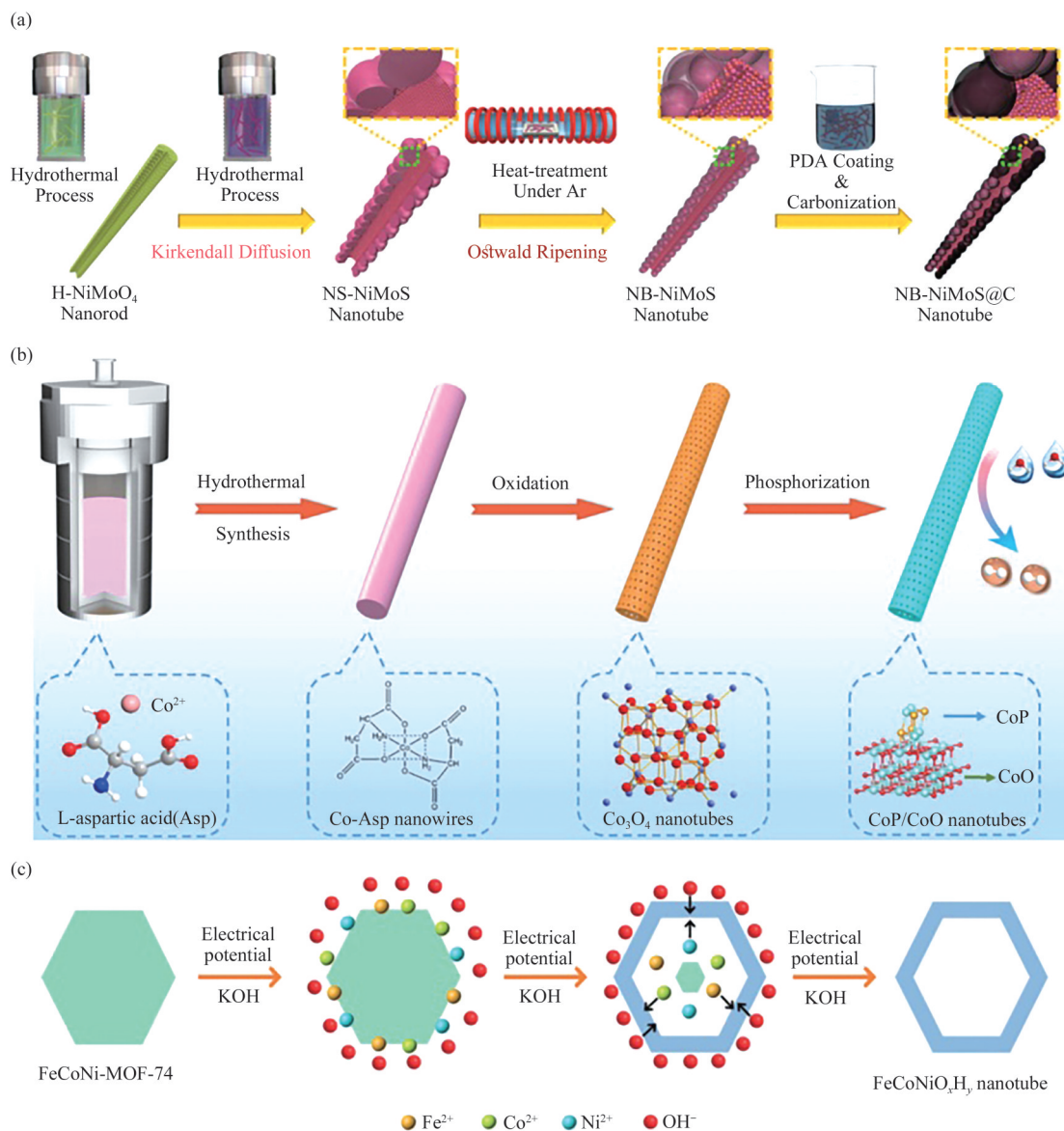
图6 Kirkendall效应下  $\text{Fe}_2\text{O}_3$  纳米棒团簇中纳米孔的形成机理

In recent years, there are some nanomaterials with novel hollow tubular structures whose electrochemical performance are superior to single hollow tubular structure<sup>[35]</sup>. CHOI *et al.*<sup>[36]</sup> demonstrated the rational design and fabrication of hierarchical tubular structures decorated with nanobubbles, which consist of multicomponent (Mo, Ni) metal sulfides (NB-NiMoS). Fig.7(a) shows their scheme, in sulfidation process, due to the diffusion of kirkendall, the outward diffusion of metal cations is faster than the inward diffusion of sulfur anions, which leads to the formation of NiS-NiS<sub>2</sub>/MoS<sub>2</sub> nanotubes. Benefiting from the rational structure and conductive N-doped carbon layers, carbon-coated NB-NiMoS (NB-NiMoS@C) exhibited excellent electrochemical performances as an anode for SIB. ZHOU *et al.*<sup>[37]</sup> demonstrated a feasible reactive template participation strategy, as shown in Fig.7(b), after mild oxidation and subsequent phosphating, the self-sacrificial template of Co-Asp nanowires was finally chemically transformed into hollow and porous CoP/CoO nanotubes. In the thermal oxidation process, Kirkendall effect was introduced to form highly hollow and porous nanotubes, which provided a large number of exposed external/internal surfaces, sufficient molecular permeability and rich electroactive sites,

greatly accelerated the reaction kinetics and improved the electrocatalytic activity. HUANG *et al.*<sup>[38]</sup> developed a new type of catalyst ( $\text{FeCoNiO}_x\text{H}_y$ ) with nanotube structure. Due to the instability of  $\text{FeCoNi-MOF-74}$  in concentrated KOH electrolyte, Fe, Co and Ni ions are released from the decomposition surface of  $\text{FeCoNi-MOF-74}$  nanorods, and react with OH<sup>-</sup> in the electrolyte to form  $\text{FeCoNiO}_x\text{H}_y$  shell as the skeleton (Fig.7(c)). At the same time, the consumption of local metal ions and OH<sup>-</sup> leads to the outward diffusion of newly released metal ions from the internally decomposed  $\text{FeCoNi-MOF-74}$ , and the inward diffusion of OH<sup>-</sup> from the external electrolyte. Finally, all fresh  $\text{FeCoNiO}_x\text{H}_y$  was formed and deposited on the surface of previously generated  $\text{FeCoNiO}_x\text{H}_y$ , which led to the formation of  $\text{FeCoNiO}_x\text{H}_y$  nanotubes.

### 2.3 2-D hollow nanostructures

In the past ten years, new methods for the controlled formation of 2D nanostructures, such nanosheets, nanoflakes, thin films and membranes have been developed. Compared with 1D nanostructures, 2D nanostructures usually exhibit better electrochemical cycling performance because the 2D feature is favorable for efficient ion and electron transport and can better accommodate the structural change during the



(a) Formation mechanism of NB-NiMoS@C nanotube (Figure adapted with permission from literature [36], copyright 2020 Elsevier B.V.); (b) Schematic illustration of the synthesis processes of CoP/CoO PNTs (Figure adapted with permission from literature [37], copyright 2022 Wiley); (c) Proposed formation process of FeCoNiO<sub>x</sub>H<sub>y</sub> nanotubes (Figure adapted with permission from literature [38], copyright 2023 Wiley)

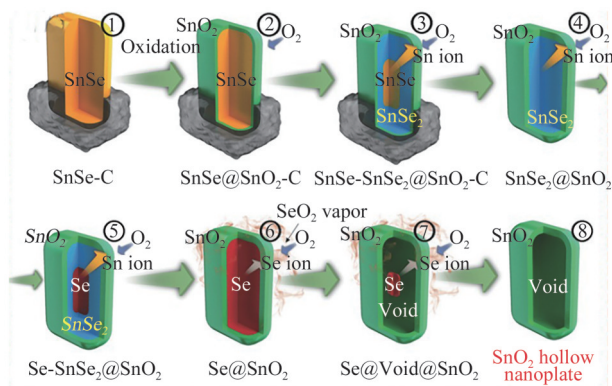
Fig. 7 Synthesis mechanism of nanotubes formed by Kirkendall effect

图 7 由 Kirkendall 效应形成的纳米管的合成机理

electrochemical reaction. In particular, their ultrathin nanosheet morphology and interconnected network structure are advantageous for efficient ion/electron transport and better accommodation of volume variation<sup>[39]</sup>.

KANG *et al.*<sup>[40]</sup> proposed a new mechanism for the transformation of nanostructured metal selenides into metal oxides *via* the Kirkendall effect. Each SnO<sub>2</sub> hollow nanoplate was transformed from a single SnSe nanoplate *via* a nanoscale Kirkendall diffusion process (Fig. 8) through core-shell structured SnSe@SnO<sub>2</sub> (Fig. 8-②), SnSe-SnSe<sub>2</sub>@SnO<sub>2</sub> (Fig. 8-③), SnSe<sub>2</sub>@SnO<sub>2</sub> (Fig. 8-④),

Se-SnSe<sub>2</sub>@SnO<sub>2</sub> (Fig. 8-⑤), Se@SnO<sub>2</sub> (Fig. 8-⑥), and yolk-shell-structured Se@void@SnO<sub>2</sub> (Fig. 8-⑦) intermediates. The complete conversion of SnSe nanoplates into SnO<sub>2</sub> by the nanoscale Kirkendall diffusion process generated the SnO<sub>2</sub> hollow nanoplates (Fig. 8-⑧). The faster diffusion rate of Sn ions (83 pm in size) relative to that of the Se ions (184 pm in size) resulted in the core-shell-structured SnSe-SnSe<sub>2</sub>@SnO<sub>2</sub>, SnSe<sub>2</sub>@SnO<sub>2</sub>, Se-SnSe<sub>2</sub>@SnO<sub>2</sub>, and Se@SnO<sub>2</sub> and yolk-shell-structured Se@void@SnO<sub>2</sub> intermediates. The SnO<sub>2</sub> hollow nanoplates exhibited uniform morphologies and



(Figure adapted with permission from literature[40],  
copyright 2017 Wiley)

Fig. 8 Formation mechanism of  $\text{SnO}_2$  hollow nanoplate *via* Kirkendall diffusion

图8  $\text{SnO}_2$ 空心纳米片的Kirkendall扩散形成机理

superior Li-ion-storage performances. The discharge capacities at 2<sup>nd</sup> and 600<sup>th</sup> cycles are 598 and 500  $\text{mAh} \cdot \text{g}^{-1}$ , respectively, and the corresponding capacity retention measured from the 2<sup>nd</sup> cycle is as high as 84%.

#### 2.4 3-D hollow nanostructures

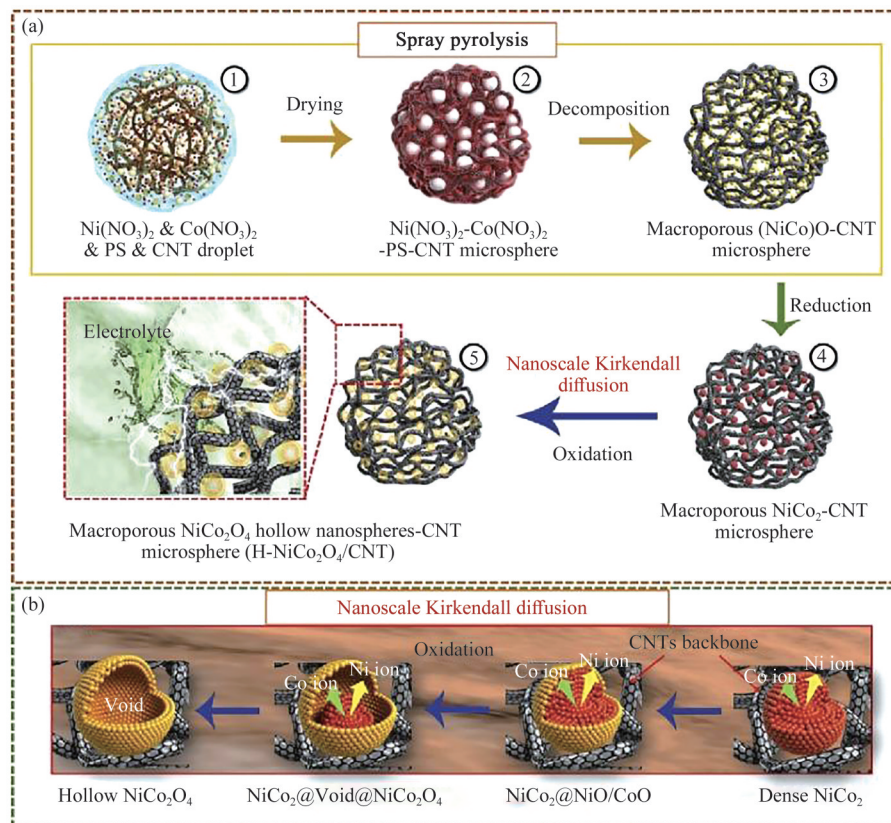
Although the single low-dimensional nanomaterial shows high capacity, due to its large surface area and energy, there are still serious self-aggregation and crushing phenomena in the cycle process, which leads to poor cycle and rate performance. In order to give full play to the advantages of nanomaterials and overcome their disadvantages, it is a promising method to construct 3-D nanostructures composed of low-dimensional nanostructure units. 3-D nanomaterials can inherit the excellent characteristics of nanostructural units, so that the materials have both high surface area and good structural stability<sup>[41]</sup>.

Hollow nanospheres with thin walls and smooth surfaces are the most common morphology of 3D nanomaterials. Thin-walled, hollow transition metal oxides have been successfully applied as anode materials for energy storage application for their unique structure, which provides an enhanced surface-to-volume ratio and a reduced transport length for both mass and charge transport. These characteristics enable the materials to have excellent electrochemical properties such as high specific capacitances, superior rate capability, and long cycle stability. PARK *et al.*<sup>[42]</sup> combined the polystyrene nanoparticle template with the nano-scale Kirkendall diffusion process and

applied them to the spray pyrolysis process to form porous  $\text{NiCo}_2\text{O}_4$ /carbon nanotube composite microspheres with extremely high rate performance as anode materials for lithium-ions battery (Fig.9(a), (b)). The surface oxidation of alloy nanocrystals leads to the formation of core-shell nanoparticles. Because of the similar size, nickel and cobalt cations diffuse to the outer surface of nanoparticles at the same time, and combine with oxygen to form NiO and CoO phases respectively. The spontaneous reaction of highly active NiO and CoO nanoclusters leads to the formation of  $\text{NiCo}_2\text{O}_4$  phase. The complete outward diffusion of Ni and Co cations transforms  $\text{NiCo}_2$  alloy nanocrystals into pure phase  $\text{NiCo}_2\text{O}_4$  hollow nanospheres.

Hollow porous nanospheres with large porosity obtained by using the nanoscale Kendall effect exhibit an obvious improvement on the cycling stability and capacity. The microporous structure of the microspheres not only act as a facile pathway for electrolyte impregnation and transport, but also protect the internal nanoparticles from aggregation and pulverization during the discharge/charge processes. PARK *et al.*<sup>[43]</sup> introduced a synthesis process of  $\text{CoSeO}_3$  microspheres with controlled morphology through the use of cobalt selenide. Partial oxidation of the  $\text{CoSe}_2$ -C composite microspheres at 400 °C in an air atmosphere yielded carbon-free  $\text{CoSeO}_3$  microspheres with ultrafine nanocrystals and high porosity *via* nanoscale Kirkendall diffusion.  $\text{CoSeO}_3$  microspheres showed a high reversible capacity of 709  $\text{mAh} \cdot \text{g}^{-1}$  in the 1400th cycle at a current density of 3  $\text{A} \cdot \text{g}^{-1}$ , and a high reversible capacity of 526  $\text{mAh} \cdot \text{g}^{-1}$  even at a very high current density of 30  $\text{A} \cdot \text{g}^{-1}$ .

3-D nanomaterials with hollow structure (yolk-shell structure, core-shell structure, multi-shell hollow structure) with special inner cavity have special advantages in the field of batteries, such as improving the contact efficiency between electrode materials and electrolytes and greatly shortening the electron/ion transmission distance. It has a stronger elastic structure, which can reduce the structural deformation in the continuous electrochemical process and is beneficial to improve the electrochemical performance. BI *et al.*<sup>[44]</sup> successfully prepared multi-Si-void @  $\text{SiO}_2$  structure by one-step oxidation of Si



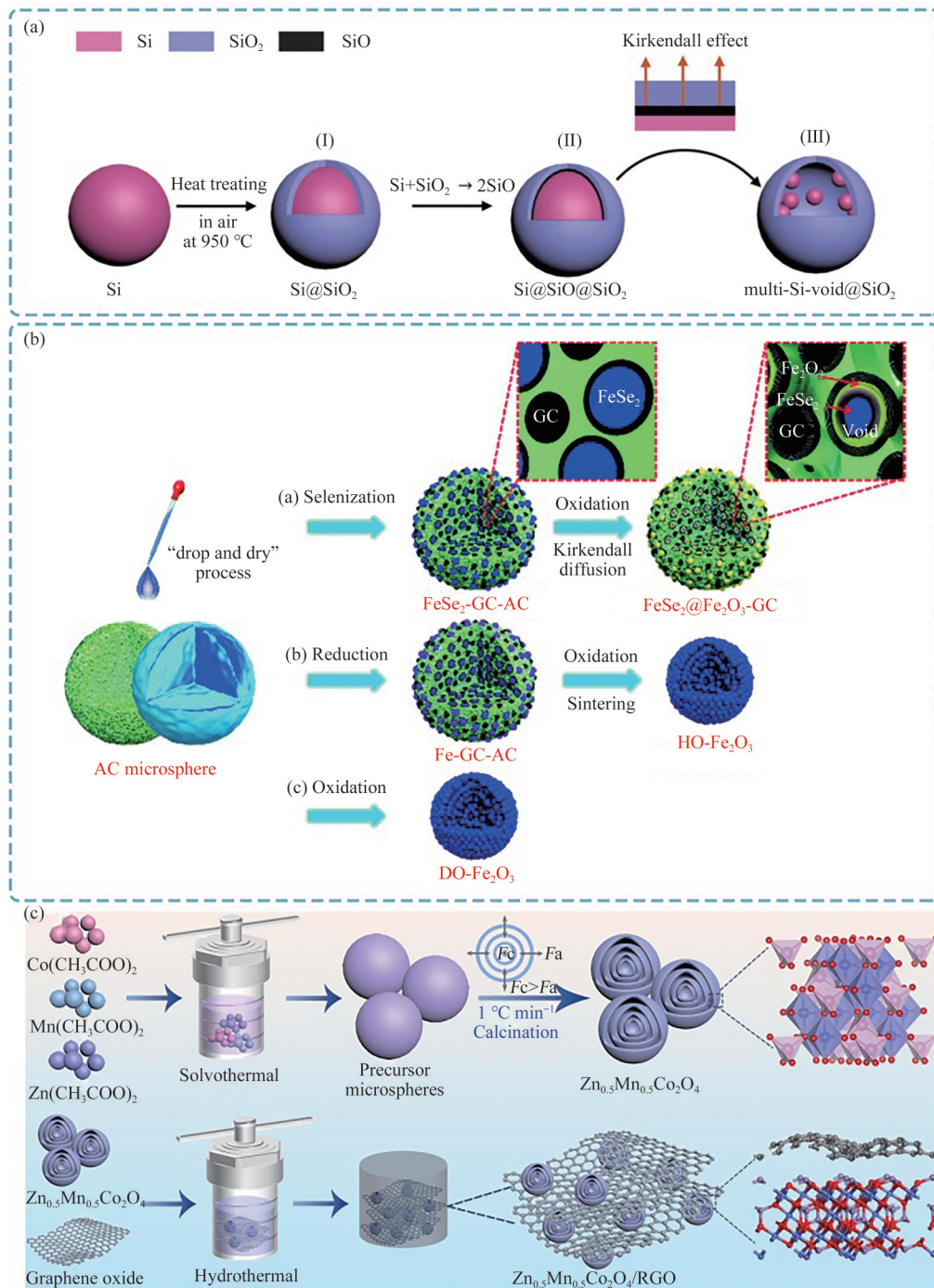
(a) Macroporous  $\text{NiCo}_2\text{O}_4$  hollow nanospheres-CNTs composite microspheres via spray pyrolysis process and two-step post-treatment process;  
 (b)  $\text{NiCo}_2\text{O}_4$  hollow nanosphere via Kirkendall diffusion (Figure adapted with permission from literature [42], copyright 2017 Elsevier Ltd.)

Fig. 9 Hollow nanospheres formed by Kirkendall effect

图9 由Kirkendall效应形成的空心纳米球

powder in air with the help of Kirkendall effect of  $\text{SiO}/\text{SiO}_2$  interface (Fig. 10 (a)). The void space and Si particle size in the structure can be adjusted by heat treatment time. The overall contact between the Si core and the  $\text{SiO}_2$  and the diffusion of Si through  $\text{SiO}_2$  shell cause the Si core to split into several smaller particles attached to the  $\text{SiO}_2$  shell. The  $\text{SiO}_2$  shell formed by direct oxidation of Si core has a good chemical bond with the core, which reduces the charge transfer barrier. The specific capacity of this material is  $1440 \text{ mAh}\cdot\text{g}^{-1}$  after 200 cycles at  $0.1 \text{ A}\cdot\text{g}^{-1}$ . As anode materials, yolk-shell structured transition-metal compounds are outstanding in enhancing the electrochemical properties on account of their structural strengths. YOO *et al.* [45] rationally designed a new type of nanostructured material that combined the advantages of metal oxides, metal selenides, and graphitic carbon (GC) as an anode material for lithium-ion batteries (Fig. 10 (b)).  $\text{FeSe}_2$  nanocrystals transformed into yolk-shell structured  $\text{FeSe}_2\text{-Fe}_2\text{O}_3$

nanospheres by nanoscale Kirkendall diffusion. Compared with the carbon-free  $\text{Fe}_2\text{O}_3$  microspheres with similar structures, the high-porosity  $\text{FeSe}_2\text{-Fe}_2\text{O}_3\text{-GC}$  microspheres have better  $\text{Li}^+$  storage performance. Designing multi-shell hollow structure is an effective method to buffer serious volume expansion and enhance charge transfer at solid-liquid interface, which can effectively improve electrochemical performance. As shown in Fig. 10 (c), YANG *et al.* [46] successfully synthesized  $\text{Zn}_{0.5}\text{Mn}_{0.5}\text{Co}_2\text{O}_4/\text{RGO}$  four-shell hollow composite. Designing the heterostructure between the four-shell hollow and RGO can generate a directional built-in electric field at the interface, thus promoting faster charge transfer and enhanced electrochemical performance. Impressively, when used as the negative electrode material of lithium-ion battery,  $\text{Zn}_{0.5}\text{Mn}_{0.5}\text{Co}_2\text{O}_4/\text{RGO}$  shows a significantly higher reversible capacity ( $1173.4 \text{ mAh}\cdot\text{g}^{-1}$  is over 100 cycles at  $0.1 \text{ A}\cdot\text{g}^{-1}$ ).

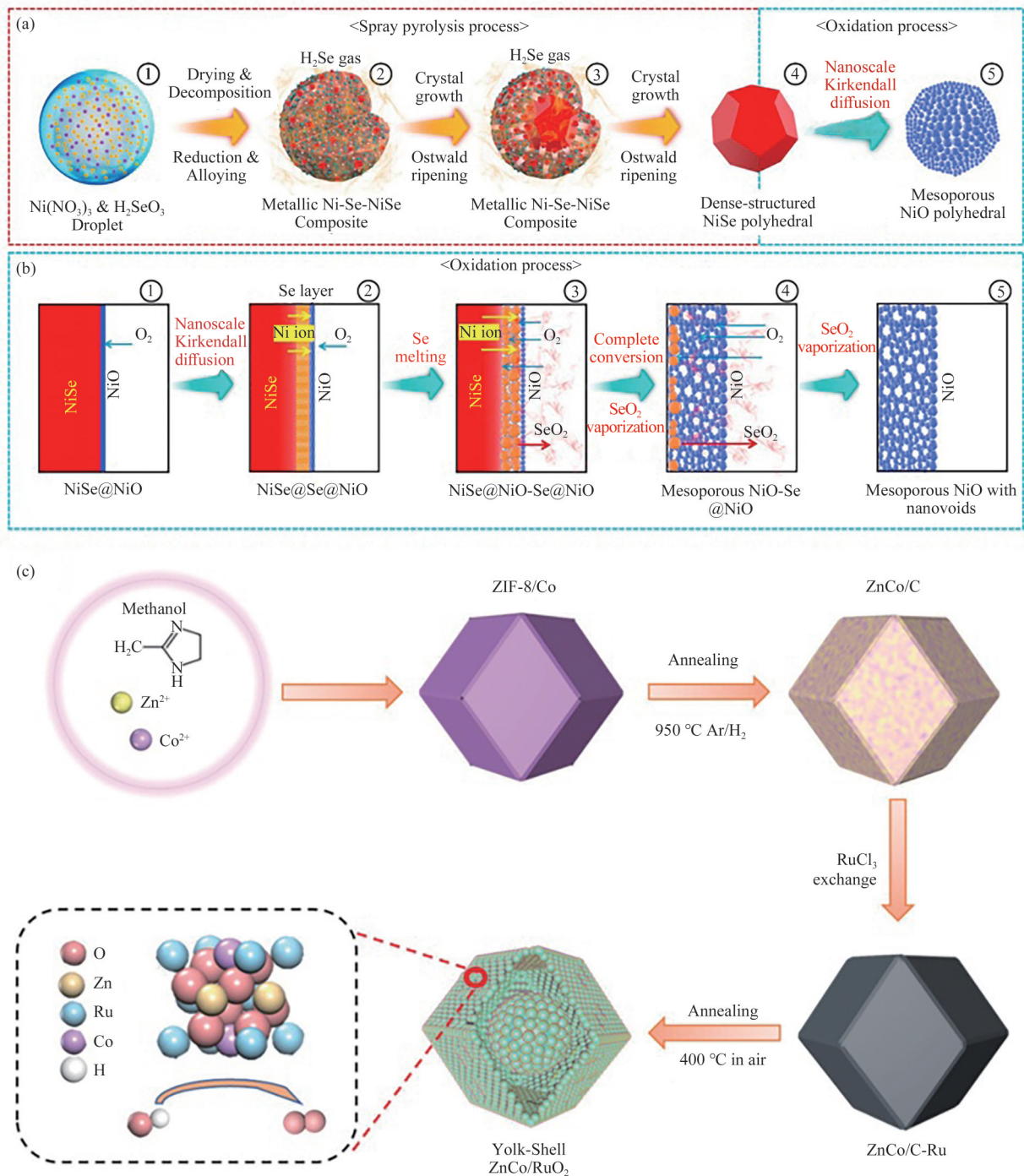


(a) Schematic illustration of the formation of multi-Si-void@SiO<sub>2</sub> structure (Figure adapted with permission from literature [44], copyright 2022 Wiley); (b) Formation mechanisms of FeSe<sub>2</sub>@Fe<sub>2</sub>O<sub>3</sub>-GC, HO-Fe<sub>2</sub>O<sub>3</sub> and DO-Fe<sub>2</sub>O<sub>3</sub> microspheres (Figure adapted with permission from literature [45], copyright 2018 The Royal of Chemistry); (c) Schematic illustration of the synthesis process and structure of quadruple-shelled hollow Zn<sub>0.5</sub>Mn<sub>0.5</sub>Co<sub>2</sub>O<sub>4</sub> and Zn<sub>0.5</sub>Mn<sub>0.5</sub>Co<sub>2</sub>O<sub>4</sub>/RGO composites (Figure adapted with permission from literature [46], copyright 2023 Elsevier B.V.)

Fig. 10 Kirkendall effect of hollow 3-D structure with special cavity  
图 10 具有特殊内腔的中空 3-D 结构的 kirkendall 效应

Except for preparation of hollow nanosphere, the nanoscale Kirkendall effect also could be introduced to grow nanocube.<sup>[47]</sup> PARK *et al.*<sup>[48]</sup> suggested a novel strategy for the synthesis of mesoporous metal oxide polyhedra with empty nanovoids by introducing

nanoscale Kirkendall diffusion into a spray pyrolysis process. To be more specific, as shown in Fig.11 (a)-(b), in the initial oxidation step, a thin NiO layer was formed on the surface of the NiSe polyhedra. The diffusion of metalloid Se into the mesopores of NiO and



(a) Formation mechanism of mesoporous NiO polyhedra by spray pyrolysis process and subsequent one-step oxidation process; (b) Formation mechanism of empty nanovoids in NiO polyhedra by Kirkendall effect (Figure adapted with permission from literature [48], copyright 2018 Elsevier B.V.); (c) Illustration of synthetic route for polyhedron-shaped yolk-shell structured ZnCo-RuO<sub>2</sub>/C assembled with ultras-small nanoparticles (Figure adapted with permission from literature [49], copyright 2023 Wiley)

Fig. 11 Kirkendall effect of nanocubes  
 图 11 纳米立方体的kirkendall效应

its reaction with oxygen gas formed SeO<sub>2</sub> nanocrystals which then evaporated into the gas phase. As a result, the step-by-step oxidation of the NiSe crystals therefore resulted in mesoporous NiO polyhedra with empty nanovoids. ZHANG *et al.*<sup>[49]</sup> prepared a polyhedral yolk

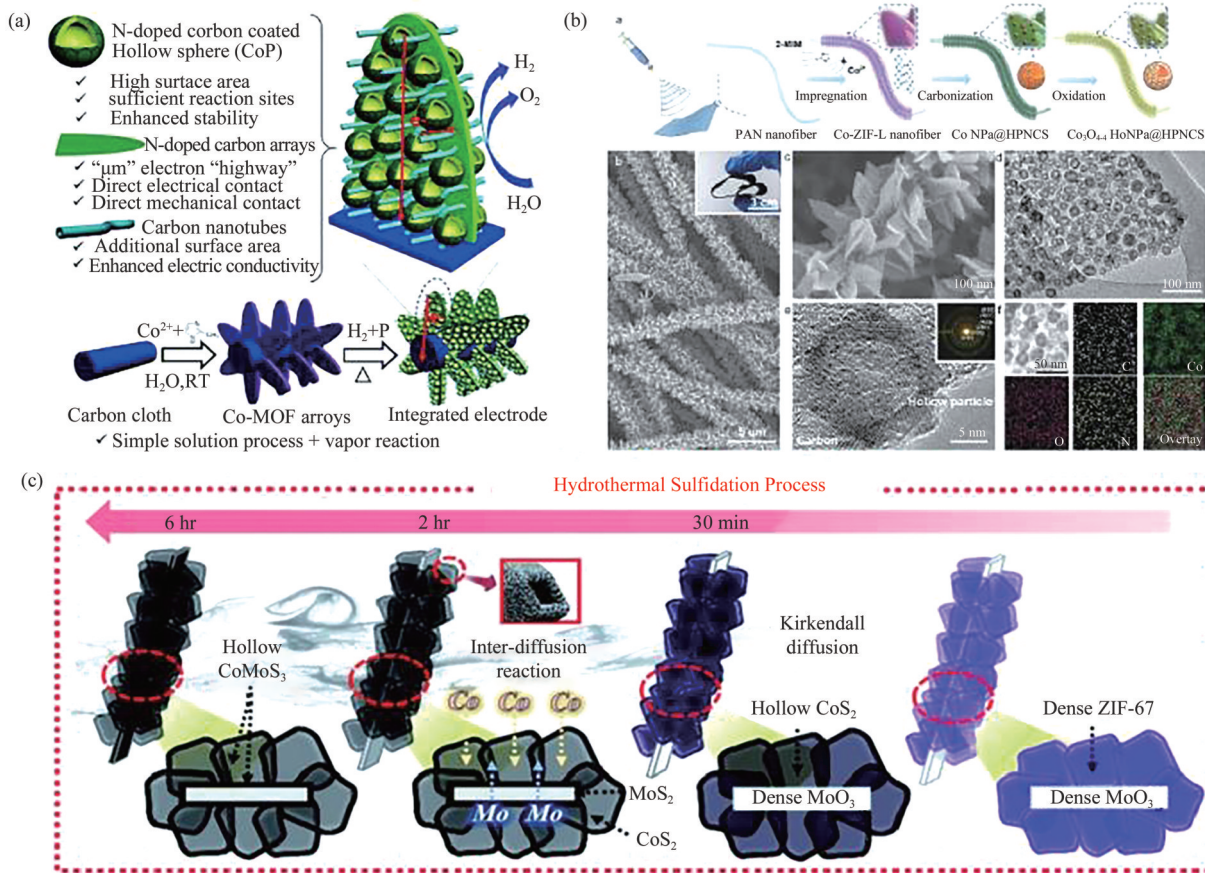
shell structure composed of zinc-cobalt-ruthenium ternary metal alloy oxide (ZnCo-RuO) by using the Kerr Kendall effect (Fig.11 (c)). The size of the yolk shell frame and the oxide nanoparticles constituting the egg yolk shell can effectively adjust the catalytic

activity and stability of the material. As the anode of zinc-air battery, ZnCo-RuO<sub>2</sub>/C shows excellent cycle performance and charge-discharge durability.

### 2.5 Composite structure

The properties of nanomaterials are largely affected by their structures, so researchers try to combine the structures of 1D, 2D and 3D together to greatly improve the performance of the nanomaterials. There are some uniformly arranged nanoarray. As shown in Fig.12 (a), GUAN *et al.*<sup>[50]</sup> demonstrated a synthetic strategy to fabricated hollow CoP nanosphere-embedded carbon nanotube/nitrogen-doped carbon (NC-CNT/CoP) nanoarrays by growing well-aligned Co-MOF nanoarrays on a carbon cloth substrate, in which a nanoscale Kirkendall effect generates few-layer graphene-coated hollow CoP nanospheres with abundant active sites. JI *et al.*<sup>[13]</sup> proposed a facile

approach (Fig.12 (b)) to controllably introduce rich oxygen vacancies into Co<sub>3</sub>O<sub>4</sub> hollow particles (Co<sub>3</sub>O<sub>4-x</sub> HoNPs). A uniform shell of ZIF-Ls with leaf-like morphology could be grown on the PAN nanofibers through a facile solution method. The ZIF-L/PAN nanofibers evolved into carbon fiber-based monolith decorated with cobalt nanoparticles (Co NPs) embedded in the vertically stacked carbon nanoflakes undergone a mild pyrolysis process. Preheat to 240 °C in air, Co NPs is oxidized through a slow Kirkendall and diffusion process to form hollow Co<sub>3</sub>O<sub>4</sub> nanoparticles with oxygen vacancies. There is also a kind of uniformly arranged nanoarray, YANG *et al.*<sup>[51]</sup> proposed a metal-organic framework-based (MOF) strategy to construct human backbone-like CoMoS<sub>3</sub> nanostructures with multiple voids as high-performance SIB anodes. As shown in Fig.12(c), as the sulfidation reaction



(a) Fabrication mechanism of hollow CoP nanosphere-embedded carbon nanotube/nitrogen-doped carbon (NC-CNT/CoP) nanoarrays (Figure adapted with permission from literature [50], copyright 2018 The Royal Society of Chemistry); (b) Synthesis procedure and TEM images of hierarchically porous N-doped carbon structure (HPNCS)(Figure adapted with permission from literature [13], copyright 2019 Wiley); (c) Schematic illustration for the formation of human backbone-like CoMoS<sub>3</sub> nanostructures(Figure adapted with permission from literature [51], Copyright 2019 The Royal Society of Chemistry)

Fig. 12 Kirkendall effect of composite nanostructures

图 12 复合纳米结构的kirkendall效应

continued, the  $\text{MoO}_3$  nanobelts also transformed into hollow  $\text{MoS}_2$  tubes *via* the Kirkendall effect, and at the same time, a solid-state reaction occurred due to interdiffusion between Mo ions in the nanobelts and Co ions in the hollow polyhedrons, resulting in the formation of  $\text{CoMoS}_3$  nanobackbones. To further improve the structural stability, the nanobackbones were coated with polydopamine to form  $\text{CoMoS}_3$ @N-doped carbon (NC) nanobackbones. Benefiting from their unique structural design, conductive carbon shells, and synergistic effects between multiple components, the  $\text{CoMoS}_3$ @NC nanobackbones exhibit enhanced electrochemical performance when tested as anode materials for SIBs. Using the Kirkendall effect, researchers also design a cluster structure formed by a large number of combinations of individual nanospheres, nanosheets or nanotubes.

### 3 Conclusions

The nanoscale Kirkendall effect based on mass transport through the interface between different solid phases, has been successfully applied for synthesizing hollow nanocrystals of various metal oxides, chalcogenides, phosphides, nitrides, and core/shell hollow structures. This paper summarizes the recent advances in hollow nanostructures ranging from nanoparticles, 1D, 2D and 3D electrodes based on nanoscale Kirkendall effect and their application in energy storage. The nanoscale Kirkendall effect takes full advantages of the interfacial reaction. There is no need to rely on external matter, but only depends on the different diffusion rate between different components to form voids.

To date, abundant applications of fabricating hollow nanomaterials using the nanoscale Kirkendall effect have been made in a common way, it is noted that the factors that affect the Kirkendall effect are needed to be further explored. There is no doubt that some internal factors of the reaction, such as reaction temperature, crystal structure, crystal defect, concentration of precursor component and so on, will affect the morphology of the final product and the size

of the cavity. Researchers should give full consideration to these factors when designing the scheme in order to obtain the required structure. In addition, researchers need to pay attention to the influence of external magnetic field on products. The macroscopic properties and microstructure of materials are closely related to the motion state of electrons. Using a strong magnetic field can make electrons and holes move freely in a specific direction. Reflected on the atom, it shows that the diffusion speed of the atom is accelerated.

In summary, hollow materials have been widely concerned and it is considered that hollow materials can greatly improve electrochemical performance because of their many active sites and large porosity which can well adapt to the volume change in the process of embedding and detaching. More and more researchers are also trying to use the Kirkendall effect to construct hollow structure materials skillfully, and a lot of remarkable achievements have been made combining with MOF, template methods, applying external energy fields and other strategies. This review can offer guidance for the design of novel hollow materials with distinguished functionalities based on the nanoscale Kirkendall effect. With an in-depth understanding for the formation mechanism, influencing factors and regulatory methods, it is promising to achieve new breakthroughs and large-scale applications in near future.

#### References

- [1] 邵雯柯,张道洪,王秋凡.基于核壳花状电极的高性能可伸缩超级电容器与光电探测器的集成(英文)[J].中南民族大学学报(自然科学版),2022,41(2):129-137.
- [2] 卢燕飞,张成江,李襄宏,等.硫氮共掺杂的片状镶嵌立方中空 $\text{TiO}_2$ 纳米晶的制备及其可见光催化性能(英文)[J].中南民族大学学报(自然科学版),2023,42(3):289-299.
- [3] WANG J, TANG H, WANG H, et al. Multi-shelled hollow micro-/ nanostructures: Promising platforms for lithium-ion batteries [J]. *Materials Chemistry Frontiers*, 2017, 1(3): 414-430.
- [4] CAO H, QIAN X, WANG C, et al. High symmetric 18-facet polyhedron nanocrystals of  $\text{Cu}_3\text{S}_4$  with a hollow

- nanocage[J]. Journal of the American Chemical Society, 2005, 127(46): 16024-16025.
- [5] HÉRAULT N, FROMM K M. Influence of the sacrificial polystyrene removal pathway on the TiO<sub>2</sub> nanocapsule structure[J]. Helvetica Chimica Acta, 2017, 100(6): e1700014.
- [6] YANG H G, ZENG H C. Creation of intestine-like interior space for metal-oxide nanostructures with a quasi-reverse emulsion[J]. Angewandte Chemie (International Ed in English), 2004, 43(39): 5206-5209.
- [7] CAO X, DAI L, WANG L, et al. A surfactant template-assisted strategy for synthesis of ZIF-8 hollow nanospheres[J]. Materials Letters, 2015, 161: 682-685.
- [8] CARUSO F, CARUSO R, MOHWALD H. Nanoengineering of inorganic and hybrid hollow spheres by colloidal templating[J]. Science, 1998, 282(5391): 1111-1114.
- [9] YANG H G, ZENG H C. Preparation of hollow anatase TiO<sub>2</sub> nanospheres via Ostwald ripening[J]. The Journal of Physical Chemistry B, 2004, 108(11): 3492-3495.
- [10] CHANG Y, TEO J J, ZENG H C. Formation of colloidal CuO nanocrystallites and their spherical aggregation and reductive transformation to hollow Cu<sub>2</sub>O nanospheres [J]. Langmuir, 2005, 21(3): 1074-1079.
- [11] HUO J, WANG L, IRRAN E, et al. Hollow ferrocenyl coordination polymer microspheres with micropores in shells prepared by Ostwald ripening [J]. Angewandte Chemie (International Ed in English), 2010, 49(48): 9237-9241.
- [12] WANG W, DAHL M, YIN Y. Hollow nanocrystals through the nanoscale Kirkendall effect[J]. Chemistry of Materials, 2013, 25(8): 1179-1189.
- [13] JI D, FAN L, TAO L, et al. The kirkendall effect for engineering oxygen vacancy of hollow Co<sub>3</sub>O<sub>4</sub> nanoparticles toward high-performance portable zinc-air batteries [J]. Angewandte Chemie (International Ed in English), 2019, 58(39): 13840-13844.
- [14] NILSSON S, ALBINSSON D, ANTOSIEWICZ T J, et al. Resolving single Cu nanoparticle oxidation and Kirkendall void formation with *in situ* plasmonic nanospectroscopy and electrodynamic simulations [J]. Nanoscale, 2019, 11(43): 20725-20733.
- [15] NAKAJIMA H. The discovery and acceptance of the Kirkendall Effect: The result of a short research career[J]. JoM, 1997, 49(6): 15-19.
- [16] YANG Z, YANG N, YANG J, et al. Control of the oxygen and cobalt atoms diffusion through co nanoparticles differing by their crystalline structure and size[J]. Advanced Functional Materials, 2015, 25(6): 891-897.
- [17] SUN Y, ZUO X, SANKARANARAYANAN S K R S, et al. Quantitative 3D evolution of colloidal nanoparticle oxidation in solution [J]. Science, 2017, 356(6335): 303-307.
- [18] GONZÁLEZ E, ARBIOL J, PUNTES V F. Carving at the nanoscale: Sequential galvanic exchange and Kirkendall growth at room temperature [J]. Science, 2011, 334(6061): 1377-1380.
- [19] LI Z, WANG J, LIU S, et al. Synthesis of hydrothermally reduced graphene/MnO<sub>2</sub> composites and their electrochemical properties as supercapacitors [J]. Journal of Power Sources, 2011, 196(19): 8160-8165.
- [20] ZHU B T, WANG Z, DING S, et al. Hierarchical nickel sulfide hollow spheres for high performance supercapacitors [J]. RSC Advances, 2011, 1(3): 397-400.
- [21] GURIA A K, PRUSTY G, PATRA B K, et al. Dopant-controlled selenization in Pd nanocrystals: The triggered Kirkendall effect [J]. Journal of the American Chemical Society, 2015, 137(15): 5123-5129.
- [22] WANG W, ZHANG P, JIANG X, et al. Constructing N-doped carbon beads-encapsulated CoMn<sub>2</sub>O<sub>4</sub> microboxes with pyramidal walls for enhanced Li storage [J]. Materials Today Energy, 2022, 30: 101149.
- [23] RAILSBACK J G, JOHNSTON-PECK A C, WANG J, et al. Size-dependent nanoscale Kirkendall effect during the oxidation of nickel nanoparticles [J]. ACS Nano, 2010, 4(4): 1913-1920.
- [24] TANG Y, ZHAO Z, HAO X, et al. Cellular carbon-wrapped FeSe<sub>2</sub> nanocavities with ultrathin walls and multiple rooms for ion diffusion-confined ultrafast sodium storage [J]. Journal of Materials Chemistry A, 2019, 7(9): 4469-4479.
- [25] HUANG Y, FANG Y, LU X F, et al. Co<sub>3</sub>O<sub>4</sub> hollow nanoparticles embedded in mesoporous walls of carbon nanoboxes for efficient lithium storage [J]. Angewandte Chemie (International Ed in English), 2020, 59(45): 19914-19918.
- [26] ZHU J, TU W, PAN H, et al. Self-templating synthesis of hollow Co<sub>3</sub>O<sub>4</sub> nanoparticles embedded in N, S-dual-doped reduced graphene oxide for lithium ion batteries [J]. ACS Nano, 2020, 14(5): 5780-5787.

- [27] FAN M, LIAO D, ABOUD M F A, et al. A universal strategy toward ultrasmall hollow nanostructures with remarkable electrochemical performance [J]. *Angewandte Chemie (International Ed in English)*, 2020, 59(21): 8247-8254.
- [28] WANG Q, MA Y, LIANG X, et al. Flexible supercapacitors based on carbon nanotube-MnO<sub>2</sub> nanocomposite film electrode [J]. *Chemical Engineering Journal*, 2019, 371: 145-153.
- [29] ZHOU G, XU L, HU G, et al. Nanowires for electrochemical energy storage [J]. *Chemical Reviews*, 2019, 119(20): 11042-11109.
- [30] LI Y, WANG Z, ZHANG Y. Ultrafine Ag/MnO nanowire-constructed hair-like nanoarchitecture: *in situ* synthesis, formation mechanism and its supercapacitive property [J]. *Journal of Alloys and Compounds*, 2015, 644: 47-53.
- [31] BANDYOPADHYAY P, SAEED G, KIM N H, et al. Fabrication of hierarchical Zn-Ni-Co-S nanowire arrays and graphitic carbon nitride/graphene for solid-state asymmetric supercapacitors [J]. *Applied Surface Science*, 2021, 542: 148564.
- [32] WANG Z, WANG H, JI S, et al. Hollow-structured NiCoP nanorods as high-performance electrodes for asymmetric supercapacitors [J]. *Materials & Design*, 2020, 193: 108807.
- [33] HUANG Y, XIE M, WANG Z, et al. All-iron sodium-ion full-cells assembled via stable porous goethite nanorods with low strain and fast kinetics [J]. *Nano Energy*, 2019, 60: 294-304.
- [34] PARK S K, CHOI J H, KANG Y C. Synthesis of hierarchical structured Fe<sub>2</sub>O<sub>3</sub> rod clusters with numerous empty nanovoids via the Kirkendall effect and their electrochemical properties for lithium-ion storage [J]. *Journal of Materials Chemistry A*, 2018, 6(18): 8462-8469.
- [35] ZHANG H, WU J, ZOU Z, et al. Create rich oxygen defects of unique tubular hierarchical molybdenum dioxide to modulate electron transfer rate for superior high-energy metal-ion hybrid capacitor [J]. *Energy & Environmental Materials*, 2023, 6(3): e12377.
- [36] CHOI J H, PARK S K, KANG Y C. N-doped carbon coated Ni-Mo sulfide tubular structure decorated with nanobubbles for enhanced sodium storage performance [J]. *Chemical Engineering Journal*, 2020, 383: 123112.
- [37] ZHOU Q, SUN R, REN Y, et al. Reactive template-derived interfacial engineering of CoP/CoO heterostructured porous nanotubes towards superior electrocatalytic hydrogen evolution [J]. *Carbon Energy*, 2023, 5(1): e273.
- [38] HUANG H, NING S, XIE Y, et al. Synergistic modulation of electronic interaction to enhance intrinsic activity and conductivity of Fe-co-Ni hydroxide nanotube for highly efficient oxygen evolution electrocatalyst [J]. *Small*, 2023, 19(36): e2302272.
- [39] CHEN D, WANG Q, WANG R, et al. Ternary oxide nanostructured materials for supercapacitors: A review [J]. *Journal of Materials Chemistry A*, 2015, 3(19): 10158-10173.
- [40] PARK G D, LEE J K, KANG Y C. Synthesis of uniquely structured SnO<sub>2</sub> hollow nanoplates and their electrochemical properties for Li-ion storage [J]. *Advanced Functional Materials*, 2017, 27(4): 1603399.
- [41] LIU P, ZHU K, GAO Y, et al. Recent progress in the applications of vanadium-based oxides on energy storage: From low-dimensional nanomaterials synthesis to 3D micro/nano-structures and free-standing electrodes fabrication [J]. *Advanced Energy Materials*, 2017, 7(23): 1770134.
- [42] PARK G D, LEE J K, KANG Y C. Three-dimensional macroporous CNTs microspheres highly loaded with NiCo<sub>2</sub>O<sub>4</sub> hollow nanospheres showing excellent lithium-ion storage performances [J]. *Carbon*, 2018, 128: 191-200.
- [43] PARK G D, HONG J H, CHOI J H, et al. Synthesis process of CoSeO<sub>3</sub> microspheres for unordinary Li-ion storage performances and mechanism of their conversion reaction with Li ions [J]. *Small*, 2019, 15(24): 1901320.
- [44] BI X, TANG T, SHI X, et al. One-step synthesis of multi-core-Void@Shell structured silicon anode for high-performance lithium-ion batteries [J]. *Small*, 2022, 18(37): 2200796.
- [45] YOO Y, HONG Y J, KANG Y C. Rationally designed microspheres consisting of yolk-shell structured FeSe<sub>2</sub>-Fe<sub>2</sub>O<sub>3</sub> nanospheres covered with graphitic carbon for lithium-ion batteries [J]. *Journal of Materials Chemistry A*, 2018, 6(31): 15182-15190.
- [46] YANG C, LI X, GAO T, et al. Novel quadruple-shelled hollow Zn<sub>0.5</sub>Mn<sub>0.5</sub>Co<sub>2</sub>O<sub>4</sub>/RGO heterostructure enable rapid and stable lithium storage performance [J]. *Chemical Engineering Journal*, 2023, 474: 145818.
- [47] GUO X, SHI J, LI M, et al. Modulating coordination of iron atom clusters on N, P, S triply-doped hollow carbon support towards enhanced electrocatalytic oxygen

- reduction [J]. *Angewandte Chemie (International Ed in English)*, 2023, 62(49): e202314124.
- [48] PARK G D, HONG J H, PARK S K, et al. Strategy for synthesizing mesoporous NiO polyhedra with empty nanovoids via oxidation of NiSe polyhedra by nanoscale Kirkendall diffusion and their superior lithium-ion storage performance [J]. *Applied Surface Science*, 2019, 464: 597-605.
- [49] ZHANG B, LUO Y, XIANG D, et al. Yolk-shell structured zinc-cobalt-ruthenium alloy oxide assembled with ultra-small nanoparticles: A superior cascade catalyst toward oxygen evolution reaction [J]. *Advanced Functional Materials*, 2023, 33(34): 2214529.
- [50] GUAN C, WU H, REN W, et al. Metal-organic framework-derived integrated nanoarrays for overall water splitting [J]. *Journal of Materials Chemistry A*, 2018, 6(19): 9009-9018.
- [51] YANG S H, PARK S K, KIM J K, et al. A MOF-mediated strategy for constructing human backbone-like CoMoS<sub>3</sub>@N-doped carbon nanostructures with multiple voids as a superior anode for sodium-ion batteries [J]. *Journal of Materials Chemistry A*, 2019, 7(22): 13751-13761.

(责编&校对 刘钊)